

## Filtering absorption and visual detection of methylene blue by nitrated cellulose acetate membrane

Shengbin He<sup>†</sup>, He Fang, and Xiaoping Xu<sup>†</sup>

College of Chemistry, Fuzhou University, Fuzhou 350108, China

(Received 20 June 2015 • accepted 6 November 2015)

**Abstract**—Wastewater-containing industrial dyes are quite harmful since most dyes are stable and toxic to humans. Detection and removing of those dyes from wastewater is necessary to ensure water supply safety. In present work, a nitrated cellulose acetate (NCA) microfiltration membrane was developed for specific absorption and visible detection of methylene blue (MB). The NCA microfiltration membrane overcomes the defect of high driven pressure in nanofiltration or ultrafiltration process. By absorption effect, the NCA membrane also overcomes the defect of low retention rate of traditional microfiltration membrane to dyes. The residual MB can be removed quickly and thoroughly by microfiltration absorption. The microfiltration membrane can also be used for visual detection of MB by concentrating the MB on membrane. The limit of detection is as low as 0.001 mg/L. The detection method is simple and free of large-scale instrument, and can be used as a portable device for spot detection of dye-contaminated water.

Keywords: Microfiltration, Cellulose Acetate, Visible Detection, Absorption, Methylene Blue

### INTRODUCTION

Water pollution caused by dye industries, including textile, plastic, leather, paper-making, cosmetics, food and dye synthesis, has gained more and more attention, since most dyes are harmful to human beings [1,2]. Wastewater-containing dyes are quite stable, which makes them difficult to biodegrade because of the complex aromatic structures of dyes [3]. Thus, the extensive uses of these dyes create not only a severe public health concern but also many serious environmental problems. Finding a way for removing dye-contaminated water effectively and thoroughly has become a hot research topic.

There are many methods employed for removing dyes from textile effluent, including coagulation, photocatalytic degradation [4], oxidative degradation [5], membrane filtration [6] and adsorption [7]. Adsorption is recognized as a more effective and economic technology among the above methods. However, in most cases, mechanical agitation is necessary to accelerate the contact between dyes and adsorbents, especially in batch absorption system. Additionally, for many adsorbents, it may consume a considerable amount of time, like 24 hours, to reach the adsorption equilibrium point [8]. Among these membrane filtration methods, pressure driven processes reverse osmosis (RO) and nanofiltration (NF) have been considered for the treatment of dye containing water from textile industry [6]. As dyes are generally small molecules, RO (driven pressure 1,000-10,000 kPa) and NF (driven pressure 500-1,500 kPa) are more suitable for treatment of industrial dye effluent. But the major drawbacks of the two membrane processes are the low flux and high operating pressure due to the small-aperture and con-

centration polarization. Ultrafiltration (UF) (driven pressure 100-1,000 kPa) operates at a lower pressure with a higher flux as compared with RO and NF, but it has a lower dye rejection than that of RO and NF. The combination of ultrafiltration and complexation ability of water soluble polymer may overcome the low retention of UF membrane while keeping the same performance of flux [9,10]. But such a combination has to introduce specific chelating agent, and the operating pressure is still high. Microfiltration (MF) (driven pressure 10-200 kPa) operates at the lowest pressure with the highest flux among all the membrane processes, but it also has a fatal flaw: with the lowest small molecule rejection.

Methylene blue (MB) is one of the most widely used substances for dyeing cotton, wood and silk. It is also commonly used in histologic and microbiologic staining. The release of MB into the water is a concern due to the toxicity, mutagenicity and carcinogenicity of the MB and its biotransformation products [11-14]. Several procedures have been reported for measurement of MB in different matrices, including UV-vis analysis, liquid-liquid extraction (LLE) and solid phase extraction (SPE) and final analysis by HPLC [15, 16]. UV-vis analysis is a relatively simple method that is the most widely used in various areas. However, the detection limit of UV-vis is about 0.1 mg/L which is relatively high [17]. Reza developed a simple and fast salting-out assisted liquid-liquid extraction followed by UV-vis spectrophotometric method and applied it for determination of MB. The limit of detection was 0.06 mg/L [16].

In the present study, we report a combination of microfiltration and absorption. A cellulose derivative microfiltration membrane was developed with the capability of adsorbing MB. The MB of trace amounts can be removed quickly and thoroughly by microfiltration absorption. The microfiltration membrane can also be used for visual detection of MB by concentrating the MB on membrane. The limit of detection is as low as 0.001 mg/L. It is believed that this pioneering work will promote the simple spot detection

<sup>†</sup>To whom correspondence should be addressed.

E-mail: comhsb@163.com, xu@fzu.edu.cn

Copyright by The Korean Institute of Chemical Engineers.

of dye contaminated waters.

## EXPERIMENTAL

### 1. Chemicals and Materials

Cellulose acetate (CA)(Guangdong Guanghua Science and Technology Co., LTD, China) was purchased from Fuzhou Bo Science Instrument Co., LTD, China. Concentrated HNO<sub>3</sub> (68%), H<sub>2</sub>SO<sub>4</sub> (98%) and other chemical reagents were all reagent grades and purchased from Fuzhou Bo Science Instrument Co., LTD.

### 2. Preparation of Cellulose Nitrate-acetate Mixed Ester

20 g CA powder was dispersed in HNO<sub>3</sub>/H<sub>2</sub>SO<sub>4</sub> with 1/1 as described by [18] with a minor modification. The mixture was magnetically stirred for a selected time at 40 °C. To optimize the reaction condition, the nitration was sustained for 1 to 10 hours. Distilled water was then added to the mixture to precipitate out the nitrated CA (NCA). The precipitate was filtered, washed repeatedly with distilled water and dried in a vacuum oven at 60 °C for 24-48 h prior to further characterization.

### 3. Preparation of Membrane

The microfiltration membrane was prepared by phase inversion method as described by [19] with minor modification. 1.5 g nitrated CA was dispersed in 8.5 ml acetone by vigorous stirring. The solution was sonicated for 2 min and left for 24 h to allow any air bubbles in the solution to dissipate. Different masses of nitrated CA were used to obtain membranes of different pore size. Native CA was also used to prepare a control membrane. Each of these bubble-free solutions was cast on a glass substrate, using a casting knife, then directly immersed in a deionized water bath kept at room temperature for phase inversion to take place by solvent/no-solvent demixing. The final thickness of the membranes was about 150 μm measured by a digital caliper with accuracy ±10 μm (Mitutoyo) at five different positions on the membrane.

### 4. Microfiltration Experiment

The filtration performance of the prepared membranes was studied by a dead-end cell filtration system connected to a nitrogen gas cylinder and solution reservoir under the pressure of 50 kPa. The membrane with effective area of 7.065 cm<sup>2</sup> was loaded into the test cell (with their dense layers facing the feed) and pressurized with double distilled water for 30 min. The pure water flux (J<sub>w</sub>, ml/min·cm<sup>2</sup>) was calculated with Eq. (1):

$$J_w = \frac{V_w}{S \Delta t} \quad (1)$$

where the parameters V<sub>w</sub>, S, and Δt represent the pure water permeate volume (ml) that passes through the membrane, membrane area (cm<sup>2</sup>) and permeation time (min).

The filtration cell and solution reservoir were refilled with 91.8 mL MB solutions (pH range of 4-8) to study the retention of the membranes to MB. The environmental temperature ranging from 16 to 35 °C was controlled by air-condition made by Haier company.

Absorption rate (Ar) was calculated by the equation:

$$Ar = \frac{A_1 - A_2}{A_1} \quad (2)$$

where A<sub>1</sub> is the absorbance of untreated dye solution and A<sub>2</sub> is the

absorbance of membrane treated dye solutions.

Absorption quantity (Aq) was calculated by the equation:

$$Aq = \frac{Ar \times C \times V}{S} \quad (3)$$

where C is MB concentration (μg/L), V is permeate MB volume (L) and S is effective area of the membrane (cm<sup>2</sup>).

### 5. Membrane Porosity

To measure the membrane porosity, wet membranes were taken out from a water bath followed by careful and quick removal of excess water on the surface by tissue paper. The wet membranes were weighted as M<sub>1</sub>, and then freeze dried overnight and weighted as M<sub>2</sub>. The water content was calculated as M<sub>1</sub>-M<sub>2</sub>. The porosity (P) was calculated as follows:

$$P = \frac{(M_1 - M_2)/q_1}{(M_1 - M_2)q_1 + M_2/q_2} \times 100 \quad (4)$$

where q<sub>1</sub> is water density and q<sub>2</sub> is NCA density.

### 6. FTIR Analysis

FTIR was conducted to characterize the chemical compositions of the original CA and nitrated CA. Infrared spectra of the samples were recorded in the range 4,000-400 cm<sup>-1</sup> on a Nicolet FTIR spectrophotometer using KBr pallets.

### 7. Characterization of Membrane Morphology

Morphological investigation of the nitrated CA and MB loaded nitrated CA. was performed using scanning electron microscopy (SEM SH-4600) with a 20 keV energy beam. The samples were sputter coated with gold prior to examination.

### 8. Preparation and Detection of Standard MB Solutions

MB of 5 mg/L was subjected to UV-vis scanning. Individual standard stock solutions of each concentration were prepared in double distilled water. MB solutions of 0.05 mg/L, 0.1 mg/L, 0.3 mg/L, 0.5 mg/L, 1 mg/L, 2 mg/L and 5 mg/L were detected by UV-vis to give a seven-point calibration curve. The MB scanning curve and scatter diagram are shown in Fig. 1. The linear regression equa-

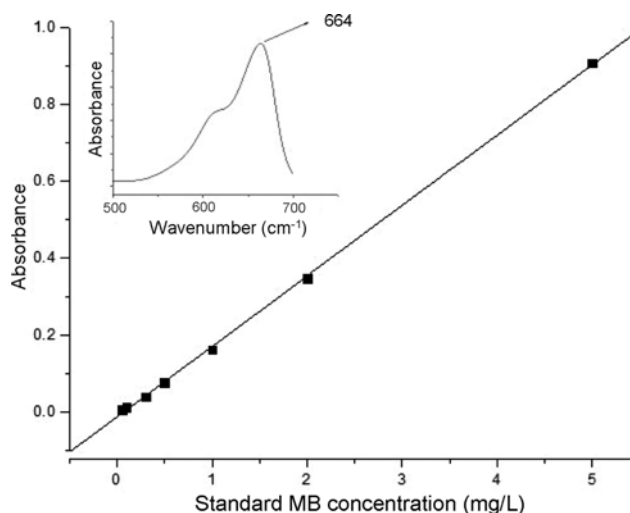


Fig. 1. Standard curve of MB concentration VS absorbance (absorption value was measured at 25 °C with distilled water as control).

tion was calculated as  $Y=0.183X-0.0118$  ( $R_2=0.9996$ ), indicating a good linear correlation.

### 9. Detection of MB by Filtration

For detection of MB solution by filtration, standard MB solutions were prepared with tap water. The NCA membrane cut into about 1 cm in diameter was loaded into a small filter with effective area of  $0.38 \text{ cm}^2$ .

## RESULTS AND DISCUSSION

### 1. Nitration of Cellulose Acetate

Among the various high polymer membranes, CA features the advantages of relative hydrophilicity, high permeating flux, wide availability and easy tunability of its chemical structure, and is widely developed for liquid separation [20-22]. But CA has low oxidation, low adsorbability and chemical affinity, which limit its further applications [23,24]. Therefore, CA derivatives made from either physical mixture or chemical modification have been investigated as a potential method of surpassing the native polymer for improved performance in various applications [25-27]. The introduction of  $-\text{NO}_2$  into CA may endow it with new functions or raise its performance.

The nitration of cellulose acetate was conducted using  $\text{HNO}_3/\text{H}_2\text{SO}_4$  with different ratio as nitration agents. In the nitration process,  $-\text{OH}$  of the cellulose acetate bonds covalently with  $-\text{NO}_2$  to form nitrate ester ( $-\text{O}-\text{NO}_2$ ).  $\text{H}_2\text{SO}_4$  acted as a catalyst in the nitration reaction and hardly reacted with cellulose acetate in the presence of  $\text{HNO}_3$  [18]. By varying the reaction time, NCAs with different degree of nitration were produced. The degree of nitration was detected by quantifying the amounts of nitrate group ( $-\text{NO}_2\%$ ). Since the only nitrogen source was from nitrate group in NCAs, the amounts of nitrogen group would be calculated from the amounts of nitrogen (N%) which was quantified by elemental analysis. As shown in Fig. 2, the degree of nitration increased with the increasing of incubation time from 1 to 8 h, and reached to as high as 12.3% ( $-\text{NO}_2$ ) when the solution was incubated for 10 hours.

### 2. IR Analysis

As shown in Fig. 3, the strong peaks in IR spectra of CA at 2,800-

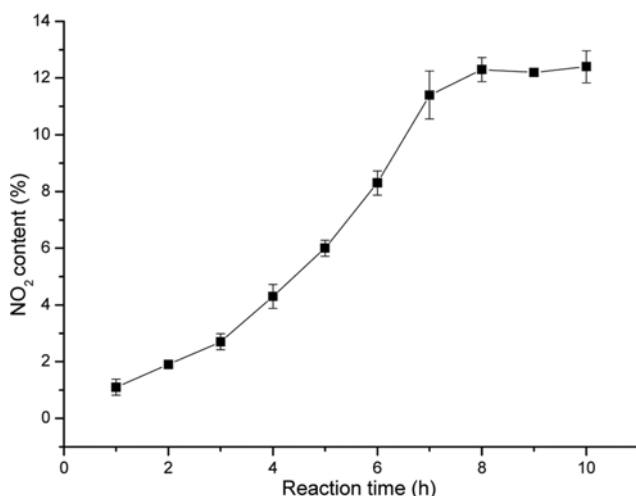


Fig. 2. The time course of nitration reaction (reaction temperature,  $40^\circ\text{C}$ ).

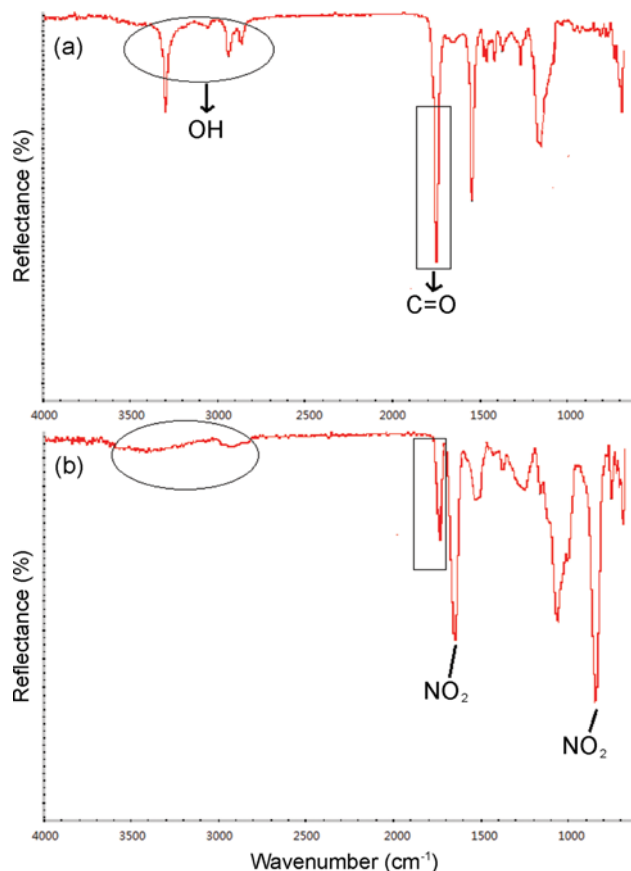


Fig. 3. FTIR of original CA and nitrated CA: (a) original CA; (b) nitrated CA ( $\text{NO}_2$  content 8.3%).

$3,400 \text{ cm}^{-1}$  appeared to be assigned to the vibration of  $-\text{OH}$  [28]. These peaks decreased in intensity or even vanished after nitration, indicating the vast consumption of  $-\text{OH}$  during the esterification process. The nitration could also be certified by the presence of new peaks at  $1,641 \text{ cm}^{-1}$  and  $840 \text{ cm}^{-1}$  which were attributed to the vibration of  $-\text{O}-\text{NO}_2$  of the cellulose nitrate. Compared with CA, the IR spectra of the NCA showed shift, enhancement or weakening in many other peaks. Some of them were attributed to the presence of  $-\text{NO}_2$ , while some were likely attributed to the several side reactions in the nitration process [18].

### 3. Influence of Nitryl Content on the Absorption of MB

In our preliminary test, we found that among the five widely used dyes (sudan III, bromophenol blue, methylene blue, crystal violet and bromocresol green), methylene blue was specially adsorbed on the nitrated CA membrane after filtration, which triggered our further study on the absorption of MB on NCA membrane. Fig. 4 shows the influence of nitryl content on the absorption of MB. The CA membrane could adsorb little amount of MB with absorption quantity of about  $2 \mu\text{g}/\text{cm}^2$ . The more the nitryl was, the higher the absorption quantity was acquired. When the  $-\text{NO}_2$  content reached to 11.4%, the absorption quantity increased to  $19.3 \mu\text{g}/\text{cm}^2$ , which is about ten times as much as native CA membrane. The absorption quantity stopped fast growing when the  $-\text{NO}_2$  content reached to 8.3%, which may be because the acquired  $-\text{NO}_2$  was nearly saturated.

With respect to absorption mechanism, few absorption routes

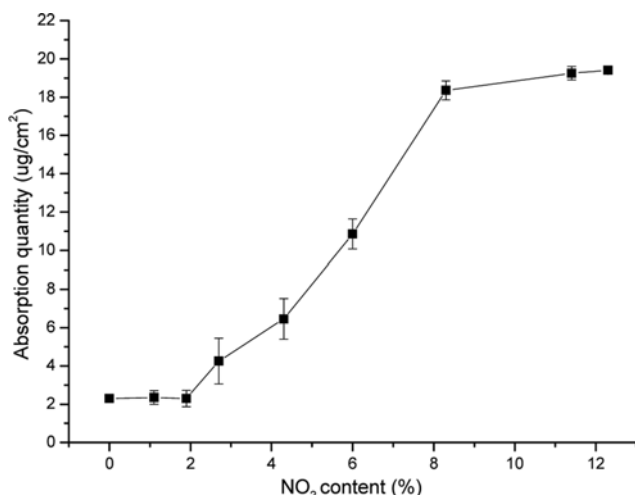


Fig. 4. Influence of NO<sub>2</sub> content on absorption quantity (MB concentration, 5 mg/L; NCA concentration, 16%; filtrate volume, 13 ml/cm<sup>2</sup>).

could be illuminated exactly. The widely accepted and applied route is electrostatic interaction of MB cations with negatively charged carbon surface functional groups [29]. Other routes such as hydrogen-bond interaction and dispersive interaction were proposed. Yavuz and Zeki reported that activated carbon could be modified by nitric acid to improve the absorption quantity of MB on activated carbon [30]. As -NO<sub>2</sub> would serve as hydrogen bond acceptors, the improved absorption ability may be ascribed to the H-bonding interactions between MB and -NO<sub>2</sub>. Although the involvement of -NO<sub>2</sub> in the absorption of MB is not illuminated definitely, both previous and present study indicated that the presence of -NO<sub>2</sub> could promote the absorption of MB.

#### 4. Influence of NCA Concentration on Properties of the Membrane

As the concentration of the membrane substrate is one of the important facts influencing the filtration properties of the membrane, NCA concentrations ranging from 6% to 20% were used to

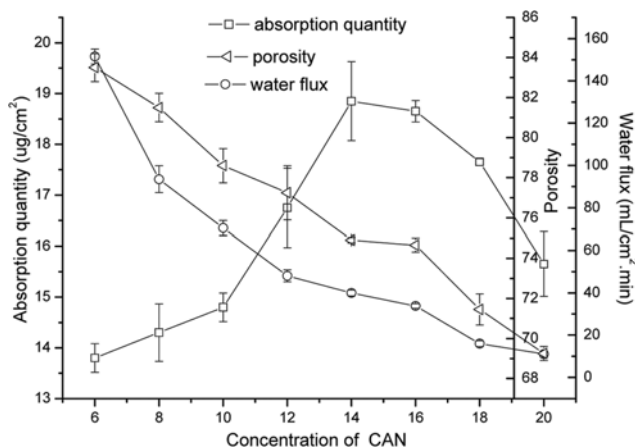


Fig. 5. Effects of NCA concentration on absorption quantity, porosity and water flux (NO<sub>2</sub> content, 8.3%; MB concentration, 5 mg/L; filtrate volume, 13 ml/cm<sup>2</sup>).

prepare microfiltration membranes. As shown in Fig. 5, both porosity and water flux had a negative relationship with the concentration of NCA. The absorption quantity increased from 13.8 μg/cm<sup>2</sup> to 18.8 μg/cm<sup>2</sup> when the NCA concentration increased from 6% to 14%. Increasing the NCA wt% further resulted in a decrease in absorption quantity. The variation of absorption quantity needs to be considered in light of changes in membrane porosity with NCA concentration. Most likely, the increasing of absorption quantity might be ascribed to the increasing of absorbing groups when low NCA concentrations were applied. When high NCA concentration was applied, the surface area decreased associated with the decreasing porosity, which then led to a decrease in absorption quantity. Generally, the higher the water flux is, the greater the efficiency and less energy consumption of the membrane. Considering all the aspects, 14% was suggested to be the optimal NCA concentration.

#### 5. The Influence of PH and Temperature on Absorption Quantity

The pH condition and temperature are considered as parameters that may affect the efficiency of dye absorption. The effect of pH and temperature on the absorption quantity of MB is illustrated in Fig. 6. In these experiments, the initial solution pH was adjusted using HCl solution (1 Mol/L) or NaOH solution (1 Mol/L) to a desired value ranging from 4 to 8 as the NCA membrane was stable in a pH range of 4-8. The results indicated that both pH (ranging from 4-8) and temperature (ranging from 16-35 °C) had no significance influence on absorption quantity of MB by NCA membrane filtration. It is suggested that variation in pH can affect the surface charge potential of the adsorbent and degree of ionization so as to affect the absorption [31,32]. The constant absorption quantity in various pH values might imply that the absorption of MB by NCA membrane had little relevance to electrostatic adsorption, or the pH variation was not wide enough to show its difference. The absorption quantity of MB by NCA membrane was also stable in temperature ranging from 16-35 °C which is controllable and economical. Thus the filtration absorption could be conducted stably in natural environment.

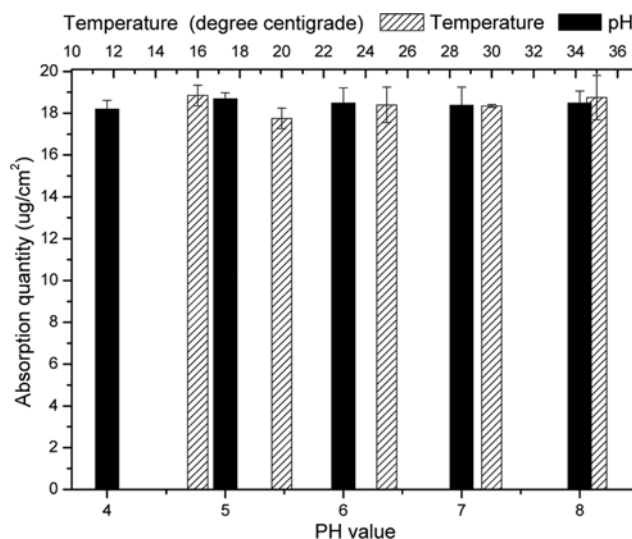


Fig. 6. Influence of pH and temperature on absorption quantity (NO<sub>2</sub> content, 8.3%; MB concentration, 5 mg/L; filtrate volume, 13 ml/cm<sup>2</sup>; NCA concentration, 14%).

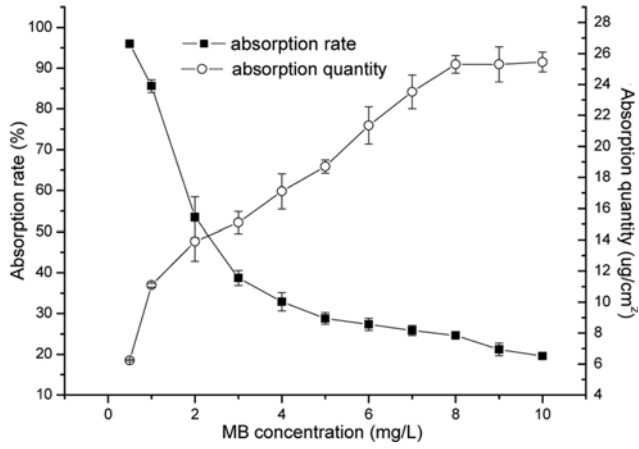


Fig. 7. Influence of MB concentration on absorption rate and absorption quantity (NO<sub>2</sub> content, 8.3%; NCA concentration, 14%; filtrate volume, 13 ml/cm<sup>2</sup>).

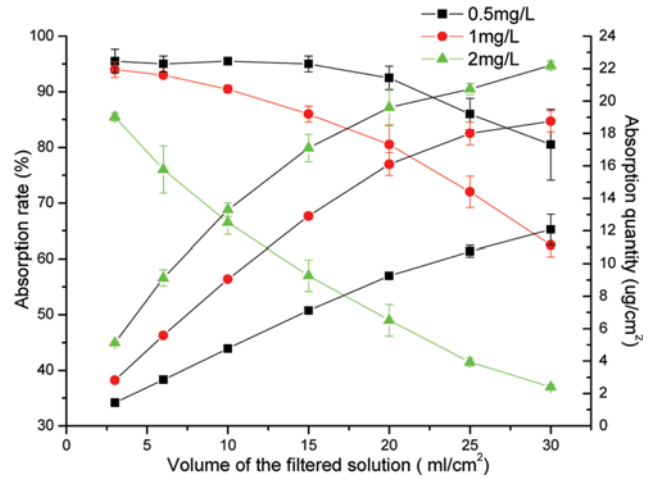


Fig. 8. Influence of filtrate volume on absorption rate and absorption quantity (NO<sub>2</sub> content, 8.3%; NCA concentration, 14%).

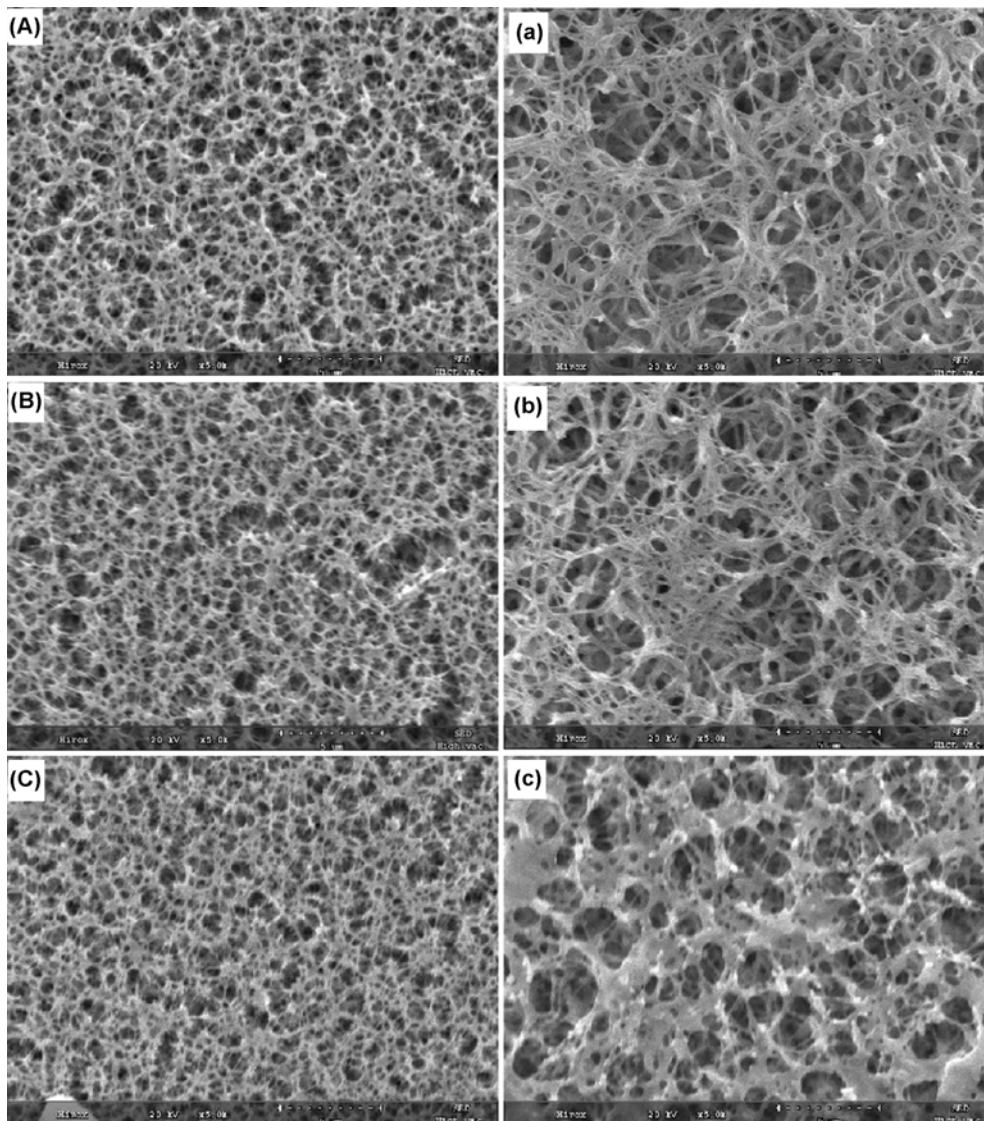


Fig. 9. Top surface (left) and under surface (right) morphologies of membranes: (A) and (a), NCA membrane; (B) and (b), MB loaded NCA membrane (6.2 mg/cm<sup>2</sup>); (C) and (c), MB loaded NCA membrane (25.3 mg/cm<sup>2</sup>).

## 6. The Influence of MB Concentration on Absorption Quantity

It is always necessary to identify the maximum saturation potential of the membrane, for which experiments should be conducted at a range of initial MB concentrations. The amount of MB absorbed on the NCA membranes quickly increased with the increasing of initial MB concentration up to 8 mg/L as seen in Fig. 7. But after this concentration, of which the absorption content reached to as high as  $25.3 \mu\text{g}/\text{cm}^2$ , the absorption of MB maintained constant, indicating saturation of the binding sites on NCA membrane. The absorption rate had a negative relationship with the initial concentration of MB. The absorption rate could reach to above 95% when low MB concentration was applied. Therefore, the present membrane could be employed either in a high concentration system to remove vast MB or in a low concentration system to purify MB contaminated water thoroughly.

## 7. The influence of Permeate Volume on Absorption Rate

Unlike traditional filtration in which target molecules are rejected through aperture-based screening, the present NCA membrane could reject MB molecules by adsorbing them on the membrane. In such a case, permeate volume together with retention (absorption rate) would be used to evaluate the clarifying capacity of the membrane to MB contaminated water. Three MB concentrations were conducted to study the clarifying capacity. As shown in Fig. 8, the membrane could reject above 90% of the MB even at a permeate volume of  $20 \text{ ml}/\text{cm}^2$  when  $0.5 \text{ mg}/\text{L}$  was applied, and could reject above 80% at the same permeate volume when  $1 \text{ mg}/\text{L}$  was applied. The MB retention was relatively low when high concentration was used. Thus, the NCA membrane would be more suit-

able for removing MB molecules thoroughly from a low concentration system.

## 8. Morphology of the Membranes

To investigate the microstructure and morphology of the NCA membranes, SEM images of the surface morphology of the samples were measured. In the phase inversion process for preparing asymmetric cellulose, it was believed that a dense selective skin is formed at the top layer (facing the air during phase inversion) of the membranes via solvent evaporation, with the rest part working as the macrovoid support [33].

Fig. 9 illustrates the morphology of the three different samples. Similar structure namely, a macrovoid support surface (under face) and a small hole sense surface (top face), can be found in the two sides of the samples. The holes on the top surface of the native NCA membrane were dense and relatively homogeneous with sizes ranging from  $0.5 \mu\text{m}$  to  $3 \mu\text{m}$  in diameter. The holes on the under surface were heterogeneous with sizes ranging from  $0.5 \mu\text{m}$  to  $5 \mu\text{m}$  in diameter. However, significant differences in morphology are noticed on both top surface and under surface after loading a large amount of MB molecules. For NCA membrane with loaded quantity of  $25.4 \mu\text{g}/\text{cm}^2$ , aperture of the top face seemed to decrease slightly. The variations in bottom surface morphology seem to result from the enormous aggregation of MB on the NCA.

## 9. Application of NCA Membrane for Visible Detection of Trace MB

So far, the detection of trace MB is dependent on a large-scale instrument which is sophisticated and needs the sample to be prepared. The most widely used method was UV-vis. Although, the

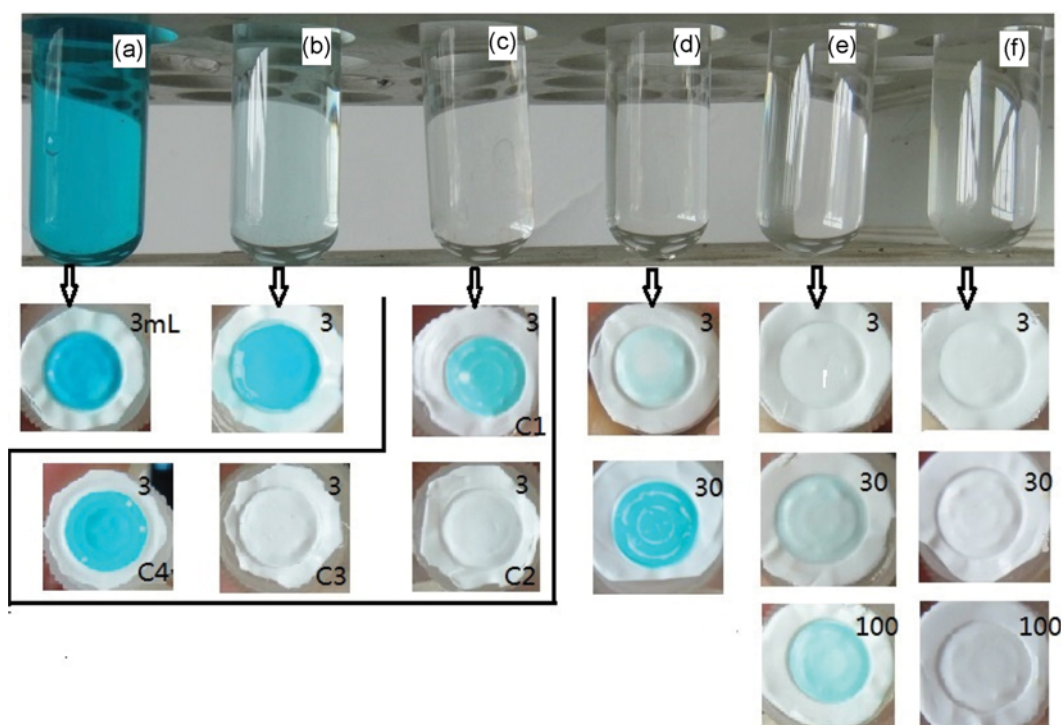


Fig. 10. Visible detection of MB by NCA membrane filtration ((a)-(e), standard MB solutions with concentrations of  $10 \text{ mg}/\text{L}$ ,  $1 \text{ mg}/\text{L}$ ,  $0.1 \text{ mg}/\text{L}$ ,  $0.01 \text{ mg}/\text{L}$  and  $0.001 \text{ mg}/\text{L}$ ; F, tap water; the number at the top right corner represents filtrate volume; C1, MB alone; C2, bromophenol blue alone; C3, crystal violet alone; C4, MB blended with bromophenol blue and violet crystal.

detection limit of UV-vis for standard MB prepared with ultrapure water can reach to 0.01-0.05 mg/L. However, such a method is limited to laboratory analysis because UV-vis is impressionable to organic pollutant. Additionally, the bulkiness of the UV-vis analyzer is not suitable for spot detection.

In the filtration of trace MB by NCA membrane, we found that MB molecules could be concentrated on the membrane to the degree of being visible. This may be applicable in the visible spot analysis of MB contaminated water. To investigate the practicability of NCA membrane in analysis of MB contaminated water, standard MB solutions prepared with tap water were used as filtrates.

The tubes in Fig. 10 show the standard MB solutions prepared with tap water. The MB solution is deep-blue for 10 mg/L, light-blue for 1 mg/L and colorless for below 0.1 mg/L. After filtering for 3 ml, the membranes were colored to be visible to the eyes for 0.1 mg/L and 0.01 mg/L. The extent of blue coloring has a positive relationship with the concentration of MB. The membrane for 0.001 mg/L was blue colored to be visible after filtering for 30 ml. Solutions containing dyes of similar color patterns were prepared to investigate the specificity of the membrane visible detection method. As shown in Fig. 10C1-4, the NCA membrane was specifically colored by MB containing solutions.

Since, the minimal visible quantity of MB adsorbed on the NCA membrane was about  $0.08 \mu\text{g}/\text{cm}^2$ . In this consistent extent of the blue coloring, the higher the MB concentration is, the less filtrate volume is needed. Therefore, the relationship between MB concentration and filtrate volume could be plotted as Fig. 11. Although the detection results are just estimates, the present analytic method is simple and free of large-scale instrument, and its detection limit is as low as 0.001 mg/L. Thus, the present method improves the detection limit by one order of magnitude as compared with the reported most accurate method [16].

## CONCLUSIONS

Nitrated cellulose acetate esters (NCA) were prepared by nitra-

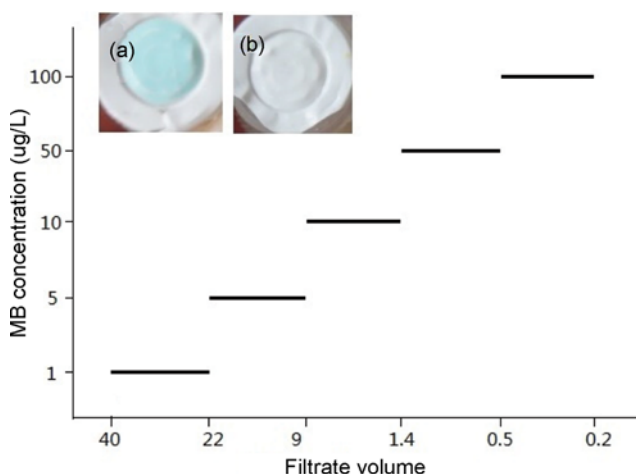


Fig. 11. The relationship between MB concentration and minimal filtrate volume ((a) slight blue with absorption quantity of about  $0.08 \mu\text{g}/\text{cm}^2$ ; (b) control group).

tion of the hydroxyl group in cellulose acetate. The formation of bone  $-\text{O}-\text{NO}_2$  was confirmed by Fourier transform infrared spectroscopy and elemental analysis. NCA-based microfiltration membranes were made and applied for specific filtration adsorption of methylene blue. Various facts influencing the absorption characteristics were investigated. The results indicated that the present membrane could be employed either in a high concentration system to remove vast MB or in a low concentration system to purify MB contaminated water thoroughly. The filtration adsorption could be conducted stably in natural environment. The NCA microfiltration membrane was also employed for visual detection of methylene blue, which is simple and free of large-scale instrument, and its detection limit is as low as 0.001 mg/L. The present analytic method has the potential to be used as a portable device for spot detection of dye contaminated water.

## ACKNOWLEDGEMENTS

The authors gratefully acknowledge financial assistance by the Specialized Research Fund for the Doctoral Program of Higher Education of China (20103514110002).

## NOMENCLATURE

### Abbreviation

CA	: cellulose
NCA	: nitrated cellulose
MB	: methylene blue
RO	: reverse osmosis
NF	: nanofiltration
UF	: ultrafiltration
MF	: microfiltration
LLE	: liquid-liquid extraction
SPE	: solid phase extraction
Jw	: pure water flux [ $\text{ml}/\text{min}\cdot\text{cm}^2$ ]
Vw	: pure water permeate volume [ml]
S	: membrane area [ $\text{cm}^2$ ]
$\Delta t$	: permeation time [min]
Ar	: absorption rate [%]
Aq	: absorption quantity [ $\mu\text{g}/\text{cm}^2$ ]
P	: porosity [%]
M	: weight

## REFERENCES

1. P. Luo, Y. F. Zhao, B. Zhang, J. D. Liu, Y. Yang and J. F. Liu, *Water Res.*, **44**, 1489 (2010).
2. F. Huang, M. Luo, L. Cui and G. Wu, *Korean J. Chem. Eng.*, **32**, 2 (2015).
3. L. Shi, G. Zhang, D. Wei, T. Yan, X. Xue, S. Shi and Q. Wei, *J. Mol. Liq.*, **198**, 334 (2014).
4. H. R. Kim, K. Y. Choi and Y. G. Shul, *Korean J. Chem. Eng.*, **24**, 4 (2007).
5. Y. Wang, X. Zhang, X. He, W. Zhang, X. Zhang and C. Lu, *Carbohydr. Polym.*, **110**, 302 (2014).
6. A. B. Fradj, S. B. Hamouda, H. Ouni, H., Lafi, R., Gzara, L. and A.

- Hafiane, S. *Purif. Technol.*, **133**, 76 (2014).
7. M. Asadullah, M. S. Kabir, M. S. Ahmed, N. A. Razak, N. S. A. Rasid and A. Aezzira, *J. Chem. Eng.*, **30**, 12 (2013).
8. Z. Karim, A. P. Mathew, M. Grahn, J. Mouzon and K. Oksman, *Carbohydr. Polym.*, **112**, 668 (2014).
9. Q. T. Nguyen, P. Aptel and J. Neel, *J. Membr. Sci.*, **6**, 71 (1980).
10. H. Strathmann, *Sep. Purif. Technol.*, **15**, 1135 (1980).
11. S. S. Auerbach, D. W. Bristol, J. C. Peckham, G. S. Travlos, C. D. Hébert and R. D. Chhabra, *Food Chem. Toxicol.*, **48**, 169 (2010).
12. A. F. Hassan, A. M. Abdel-Mohsen and M. M. F. Fouda, *Carbohydr. Polym.*, **102**, 192 (2014).
13. Y. Hirak, H. Goto, M. Kohno, D. Kawanishi and M. Murata, *BBA*, **1840**, 2776 (2014).
14. A. Petzer, B. H. Harvey, G. Wegener, J. P. Petzer and B. Aure, *Appl. Pharm.*, **258**, 403 (2012).
15. L. Sun, A. M. Reddy, N. Matsuda, A. Takatsu, K. Kato and T. Okada, *Analytica Chimica Acta*, **487**, 109 (2003).
16. R. S. Razmara, A. Daneshfar and R. Sahrai, *J. Ind. Eng. Chem.*, **17**, 533 (2011).
17. N. Bélaz-David, L. A. Decosterd, M. Appenzeller, Y. A. Ruetsch, R. Chioleró, T. Buclin and J. Biollaz, *Eur. J. Pharm. Sci.*, **5**, 335 (1977).
18. L. Li and M. Frey, *Polymer*, **51**, 3774 (2010).
19. N. E. Badawi, A. R. Ramadan, A. M. K. Esawi and M. El-Morsi, *Desalination*, **344**, 79 (2014).
20. M. Hayama, K. Yamamoto, F. Kohori and K. Sakai, *J. Membr. Sci.*, **234**, 41 (2004).
21. A. Idris and L. K. Yet, *J. Membr. Sci.*, **280**, 920 (2006).
22. D. Wang, X. Zhang and J. Diniz da Costa, *J. Membr. Sci.*, **454**, 119 (2014).
23. B. Han, D. Zhang, Z. Shao, L. Kong and S. Lv, *Desalination*, **311**, 80 (2013).
24. R. Lia, L. Liu and Yang, *J. Hazard. Mater.*, **280**, 20 (2014).
25. C. M. Kee and Idris, *J. Ind. Eng. Chem.*, **18**, 2115 (2012).
26. A. A. Qaiser, M. M. Hyland and D. A. Patterson, *Synth. Met.*, **162**, 958 (2012).
27. H. Wua, B. Unnikrishnana and C. Huang, *Sensor. Actuat. B*, **203**, 880 (2014).
28. S. Rajam and C. Ho, *J. Membr. Sci.*, **281**, 211 (2006).
29. J. Guo, B. Li, L. Liu and K. Lv, *Chemosphere*, **111**, 225 (2014).
30. Y. Gokce and Z. Aktas, *Appl. Surf. Sci.*, **313**, 352 (2014).
31. Y. F. Lin, H. W. Chen, P. S. Chien, C. S. Chiou and C. C. Liu, *J. Hazard. Mater.*, **185**, 1124 (2011).
32. R. Mukherjee and S. De, *J. Hazard. Mater.*, **265**, 8 (2014).
33. S. Zhang, K. Y. Wang, T. Chung, Y. C. Jean and H. Chen, *Chem. Eng. Sci.*, **66**, 2008 (2011).